Kinetics and Mechanism of Phosphine Exchange for Ruthenium(II) Complexes in the Series $(\eta^5\text{-}C_5Me_5)(PMe_3)_2RuX$. Ancillary Ligand Effects on Dative Ligand Dissociation

Henry E. Bryndza,*[,1] Peter J. Domaille,[1] Rocco A. Paciello,[2] and J. E. Bercaw*[,2]

Central Research and Development Department of the E. I. DuPont de Nemours & Co., Inc.,† Experimental Station, Wilmington, Delaware 19898, and Division of Chemistry and Chemical Engineering, California Institute of Technology,‡ Pasadena, California 91125

Received February 11, 1988

Dissociative trimethylphosphine exchange kinetics have been studied for the complexes $Cp^*(PMe_3)_2RuX$ ($Cp^* = \eta^5\text{-}C_5Me_5$; X = NPh_2, NHPh, OH, SPh, OPh, SH, Cl, Br, CH_2SiMe_3, CH_2COCH_3, I, Ph, CH_2Ph, CH_3, CCPh, H). Activation parameters for phosphine dissociation have been obtained for all complexes; these parameters make it possible to evaluate both the steric and electronic contributions to phosphine ligand dynamics for ancillary ligands X. Activation enthalpies for phosphine dissociation, which approximate Ru–P bond dative strengths (assuming similar barriers for PMe_3–$[Cp^*(PMe_3)RuX]$ recombination), show a marked dependence on the steric requirements of X. The substantial variation in activation enthalpies found among the various ancillary X ligands suggests the functional group additivity approach to organometallic thermochemistry may have limited applicability. In addition, lone electron pairs on X (e.g. for X = OH) substantially stabilize the transition state for such dative ligand loss and dramatically accelerate phosphine dissociation in comparison to complexes having alkyl ligands of about the same size (e.g. X = CH_3).

Introduction

An appreciation of the strength of transition metal-to-ligand bonds (M–L and M–X bond dissociation energies (BDEs) for $L_nM\text{–}X_m$ complexes; L = "datively" bonded donor ligand, X = "normal covalently" bonded σ ligand) is of unquestioned importance to an understanding of the reactivity and mechanisms involving organotransition-metal and coordination compounds. We have recently reported an apparently general one-to-one correlation between the relative $L_nM\text{–}X$ bond dissociation energies for organoruthenium and organoplatinum compounds of the types $Cp^*(PMe_3)_2Ru\text{–}X$ and $(Ph_2PCH_2CH_2PPh_2)(CH_3)\text{-}Pt\text{–}X$ (X = NPh_2, NHPh, OH, SPh, OPh, SH, Cl, Br, CH_2SiMe_3, CH_2COCH_3, I, Ph, CH_2Ph, CH_3, CCPh, H) and the corresponding H–X BDEs.[3] The assumption inherent in the evaluation of these data (K_{eq} for eq 1), as well as

$$Cp^*(PMe_3)_2Ru\text{–}X + H\text{–}Y \underset{}{\overset{K_{eq}}{\rightleftharpoons}} Cp^*(PMe_3)_2Ru\text{–}Y + H\text{–}X \quad (1)$$

in virtually every other solution-phase thermochemical investigation into organotransition-metal chemistry,[4] has been the principle of functional group thermochemical additivity,[5] which has proven so convenient in organic systems. While it seems reasonable that the Ru–P bonds in $Cp^*(PMe_3)_2Ru\text{–}X$ will be about as strong as those in $Cp^*(PMe_3)_2Ru\text{–}Y$, this assumption has never been tested for organometallic systems.

In order to assess the validity of this assumption for a representative series of $L_nM\text{–}X$ compounds, we elected to establish the relative dative bond dissociation enthalpies for this series of $Cp^*(PMe_3)(X)Ru\text{–}PMe_3$ complexes to evaluate how changes in steric requirements of ancillary X σ ligands affect Ru–P bond dissociation enthalpies. Similar measurements on complexes containing lone electron pairs on X were also made to determine how effective various substituents can be in stabilizing (formally) 16-electron unsaturated intermediates $[Cp^*(PMe_3)RuX]$ for complexes with similar steric constraints.

Phosphine dissociation from organometallic complexes has been studied as a means of estimating M–L bond strength for a number of other systems.[6] Generally, these studies have involved measuring equilibria[7] of the type

$$L_nM \underset{k_1}{\overset{k_1}{\rightleftharpoons}} [L_{n-1}M] + L \quad (2)$$

The effects of varying the steric bulk of L on the rates of dissociation (k_1) and the extent of dissociation (k_1/k_1) have been examined. There have also been numerous studies of the effects of trans labilizing, σ-bonded ligands on M–L bond strengths for "classical" coordination complexes.[8] On the other hand, to our knowledge no studies have been conducted of ligand loss from an organometallic complex as the ancillary ligand X is systematically varied. To the extent that the barrier for recombination of $[Cp^*(PMe_3)RuX]$ and PMe_3 remains relatively small and constant, the $Ru\text{–}PMe_3$ dative BDEs are approximated by the enthalpies of activation for phosphine loss so obtained.

We have previously shown that the phosphine ligands in $Cp^*(PMe_3)_2RuX$ complexes are thermally labile and that loss of PMe_3 leads to formation of very reactive, coordinatively unsaturated species, $[Cp^*(PMe_3)RuX]$, capable of arene C–H bond activation.[9] We have also ob-

† Contribution no. 4546.
‡ Contribution no. 7736.

(1) E. I. du Pont de Nemours and Co., Inc., Central Research and Development Department.
(2) Division of Chemistry and Chemical Engineering, California Institute of Technology.
(3) Bryndza, H. E.; Fong, L. K.; Paciello, R. A.; Tam, W.; Bercaw, J. E. *J. Am. Chem. Soc.* **1987**, *109*, 1444.
(4) See, for example, the special issue of *Polyhedron*, Symposium in Print: "Metal-Ligand Bonding Energetics in Organotransition Metal Compounds", Marks, T. J., Ed.
(5) Sometimes called the "Benson Approximation" in reference to the successful approach to organic thermochemistry outlined in: Benson, S. W. *Thermochemical Kinetics*, 2nd ed.; Wiley-Interscience: New York, 1976.
(6) For an overview see: Tolman, C. A. *Chem. Rev.* **1977**, *77*, 313.
(7) Martinho Simoes, J. A.; Beauchamp, J. L. *Chem. Rev.*, in press.
(8) See, for example: Langford, C. H.; Gray, H. B. *Ligand Substitution Processes*; W. A. Benjamin: Reading, MA, 1966.
(9) Tilley, T. D.; Togni, A.; Paciello, R. A.; Bercaw, J. E.; Grubbs, R. H., manuscript in preparation.

0276-7333/89/2308-0379$01.50/0

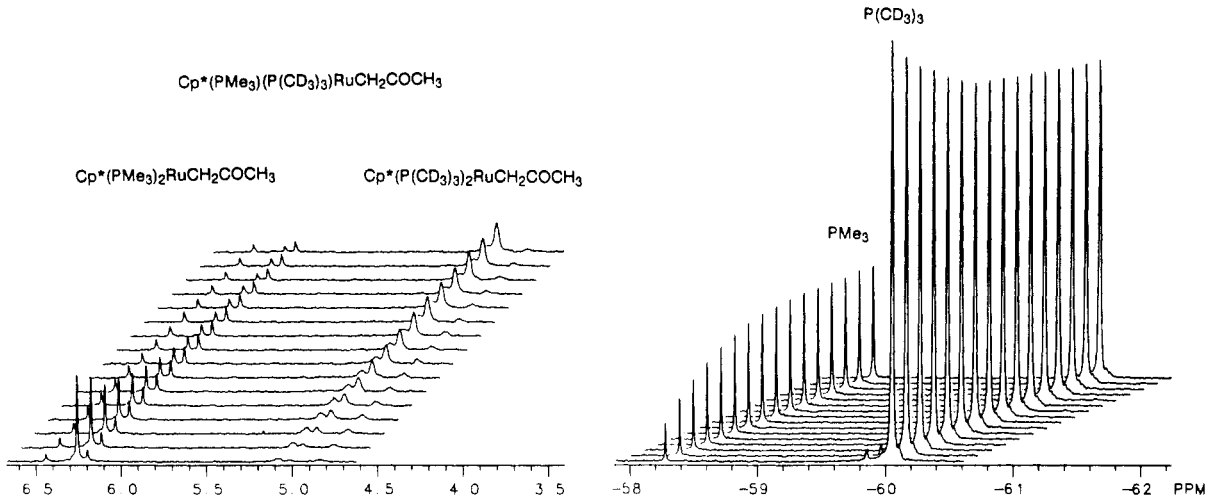

Figure 1. A. The Ru–P region of ^{31}P NMR spectra taken during a reaction of $Cp^*(P(CH_3)_3)_2RuCH_2COCH_3$ with $P(CD_3)_3$ at 100 °C. Note the sharp singlet corresponding to starting material, the doublet of doublets corresponding to $Cp^*(P(CH_3)_3)(P(CD_3)_3)RuCH_2COCH_3$, and the broad singlet corresponding to $Cp^*(P(CD_3)_3)_2RuCH_2COCH_3$ are all distinguishable at 121 MHz. The Ru–$P(CH_3)_3$ and Ru–$P(CD_3)_3$ are easily integrated by standard techniques. B. The PMe_3 region of ^{31}P NMR spectra taken during a reaction of $Cp^*(PCH_3)_3)_2RuCH_2C_6H_5$ with $P(CD_3)_3$ at 100 °C. Singlets for $P(CD_3)_3$ and $P(CH_3)_3$ are easily integrated by standard techniques.

served that these phosphine ligands are photochemically labile and that when irradiated $Cp^*(PMe_3)_2Ru$–R (R = H, alkyl) compounds generate species capable of activating even the C–H bonds of aliphatic hydrocarbons.[10] Preliminary studies of these reactions have shown a strong inhibition of the overall reaction by excess phosphine which implies that phosphine dissociation precedes the rate-determining step of the C–H bond oxidative addition.[11] Moreover, the electronic structure proposed for the complexes of the type Cp^*L_2MX (M = Ru, Fe; L = PMe_3, PEt_3, CO; X = hydride, halide, alkyl, aryl) is indicative of an excited state which is antibonding with respect to [Ru–P], so that the reactive species $[Cp^*(PMe_3)(X)Ru]$ is expected to be accessible upon broadband photochemical excitation.[12] Indeed, phosphine loss appears to dominate the chemistry of these $Cp^*(PMe_3)_2RuX$ complexes, yet it is still not clear what factors govern these "simple" phosphine dissociation processes.

We report herein activation parameters obtained by studying ligand dissociation in the complexes $Cp^*(PMe_3)(X)Ru$–PMe_3 and an interpretation of the trends observed on varying X.

Results

The availability of such a wide range of ruthenium complexes of the type $Cp^*(PMe_3)_2RuX$ (X = NPh_2, NHPh, OH, SPh, OPh, SH, Cl, Br, CH_2SiMe_3, CH_2COCH_3, I, Ph, CH_2Ph, CH_3, CCPh, H)[3,13] would appear to make a study of these phosphine substitution process quite straightforward. On the other hand, there are certain limitations to the traditional kinetic treatment of a system undergoing reversible loss of PMe_3 according to eq 3. The method of initial rates for approach to equilibrium or use of a large excess of PMe_3 to achieve pseudo-first-order kinetics, assumes that the trapping rate (k_{-1}) is very much faster than the dissociation rate, k_1, and is irreversible. These methods generally do not take into account that the approach of the entire system, mono- and bis-labeled

$$Cp^*(PMe_3)_2Ru\text{–}X \underset{k_{-1}}{\overset{k_1}{\rightleftharpoons}} [Cp^*(PMe_3)Ru\text{–}X] + PMe_3 \quad (3)$$

$$[Cp^*(PMe_3)Ru\text{–}X] + {}^{\ddagger}PMe_3 \underset{k_1}{\overset{k_{-1}}{\rightleftharpoons}} Cp^*(PMe_3)({}^{\ddagger}PMe_3)Ru\text{–}X$$

$$Cp^*(PMe_3)({}^{\ddagger}PMe_3)Ru\text{–}X \underset{k_{-1}}{\overset{k_1}{\rightleftharpoons}} [Cp^*({}^{\ddagger}PMe_3)Ru\text{–}X] + PMe_3$$

$$[Cp^*({}^{\ddagger}PMe_3)Ru\text{-}X] + {}^{\ddagger}PMe_3 \underset{k_1}{\overset{k_{-1}}{\rightleftharpoons}} Cp^*({}^{\ddagger}PMe_3)_2Ru\text{–}X$$

$Cp^*(PMe_3)_2RuX$, free phosphine (PMe_3), and free labeled phosphine ($^{\ddagger}PMe_3$), to equilibrium must be considered. Experimentally, use of ^1H or ^2H NMR and a labeled phosphine such as $P(CD_3)_3$ does not allow the concentrations of all components in the system to be quantitatively determined.[14] Such considerations suggested to us the use of ^{31}P NMR as the proper analytical technique, and multiparameter fitting of a suitable kinetic model of the resultant data as a method of extracting the dissociation rate constant (k_1) of interest.

Initial efforts to examine ligand exchange processes in $Cp^*(PMe_3)_2RuSPh$ via ^{31}P NMR utilized $^{13}CH_3PMe_2$ as the labeled phosphine ($^{\ddagger}PMe_3$ in eq 3). We observe that the $^1J_{C\text{-}P}$ (of ca. 13 Hz) in ruthenium complexes which contain $^{13}CH_3PMe_2$ is too small to reliably resolve and integrate resonances corresponding to the metal-bound labeled and unlabeled ligand signals. However, signals corresponding to the free phosphines in solution may be quantitatively determined, and some preliminary observations were therefore possible. Pseudo-first-order reaction conditions, in which 10 equiv of added $^{13}CH_3PMe_2$ were used, showed PMe_3 exchange rates only incrementally slower than for a similar experiment involving the use of

(10) Merola, J.; Bercaw, J. E., unpublished results.
(11) Tilley, T. D.; Togni, A.; Bercaw, J. E.; Grubbs, R. H., unpublished results.
(12) Bray, R. G.; Bercaw, J. E.; Gray, H. B.; Hopkins, M. D.; Paciello, R. A. *Organometallics* **1987**, *6*, 922.
(13) Tilley, T. D.; Grubbs, R. H.; Bercaw, J. E. *Organometallics* **1984**, *3*, 274.

(14) The concentrations of labeled free $P(CD_3)_3$ cannot be determined in this system by simple integration, and estimates of this quantity by difference suffer from not taking into account the rates (or final levels) of phosphine leaving the solution for the gas phase. Neither can the assumption that this effect will be constant for all systems studied be made; obtaining activation parameters for even one derivative requires rate studies at a variety of temperatures. The $PMe_3(soln) \rightleftharpoons PMe_3(g)$ equilibrium clearly depends on temperature (vide infra). These limitations require the accurate determination of all important solution phase concentrations by ^{31}P NMR.

20 equiv of this phosphine. Such "saturation kinetics" strongly suggest ligand exchange in these ruthenium complexes proceeds via a dissociative pathway. In addition, the amount of free phosphine in solution could be monitored against an internal standard as a function of temperature, and it was observed that significant amounts had migrated into the gas phase (ca. 20% after 2 half-lives at 100 °C).

Ligand exchange reactions were then studied by the addition of $P(CD_3)_3$ to unlabeled $Cp^*(PMe_3)_2RuX$ complexes. A large isotopic shift was observed in the ^{31}P NMR for perdeuteriated and perproteated phosphine (0.9 ppm at 100 °C), and the spectral features of Ru–PMe_3 and Ru–$P(CD_3)_3$ functional groups were found to be similarly well resolved (Figure 1). However, large differences were observed in the ^{31}P NOE enhancements for labeled vs unlabeled phosphines when conventional "1 pulse" Fourier transform techniques were used; a factor of ca. 2.5 was noted for the intensity of the signal for PMe_3 vs $P(CD_3)_3$. In addition, long spin–lattice relaxation values (T_1s) of 5–15 s have been measured for the ^{31}P signals of $Cp^*(PMe_3)_2RuX$ complexes, so long delays between acquisition pulses must be used to obtain spectra where integrals accurately reflect concentrations of individual species in solution.[15]

These observations led to the final experimental design. The concentrations of metal-bound labeled and unlabeled phosphine and free labeled and unlabeled phosphine were measured as a function of time at a given temperature by ^{31}P NMR. Quantitative results were obtained by using an NOE suppressed kinetics pulse sequence[16] and by using 60-s (ca. 4–5 T_1s) pulse delays. By measuring the initial weights of $Cp^*(PMe_3)_2RuX$ (no more than 5% loss of metal complex was ever observed) and $P(CD_3)_3$, the amount of each phosphine migrating to the gas phase ($PMe_{3(g)}$ and $P(CD_3)_{3(g)}$) could be calculated as a function of time.

The acquired data were numerically integrated by an iterative process to the following kinetic model (eq 4) which incorporates dissociative ligand exchange with simultaneous liquid- to gas-phase phosphine equilibrium.[17] The

$$Cp^*(PMe_3)XRu\text{–}PMe_3 \underset{k_{-1}}{\overset{k_1}{\rightleftharpoons}} [Cp^*(PMe_3)XRu] + PMe_3 \{PMe_3 = P(CH_3)_3\} \quad (4)$$

$$Cp^*(PMe_3)XRu\text{–}P(CD_3)_3 \underset{k_{-1}}{\overset{k_1}{\rightleftharpoons}} [Cp^*(PMe_3)XRu] + P(CD_3)_3$$

$$PMe_{3(soln)} \underset{k_2}{\overset{k_2}{\rightleftharpoons}} PMe_{3(g)}$$

$$P(CD_3)_{3(soln)} \underset{k_{-2}}{\overset{k_2}{\rightleftharpoons}} P(CD_3)_{3(g)}$$

assumption made in this method of obtaining dissociation rate constants is that the rates for these processes do not change upon isotopic labeling. Support for this assumption comes from finding the anticipated equilibrium constants (K_5) of 1.00 (5) for the final equilibrium mixtures (eq 5).

$$Cp^*(PMe_3)\{P(Cy_3)\}Ru\text{–}X + P(CD_3)_3 \overset{K_5}{\rightleftharpoons} Cp^*\{P(CD_3)_3\}\{P(Cy_3\}Ru\text{–}X + PMe_3 \quad Y = H, D) \quad (5)$$

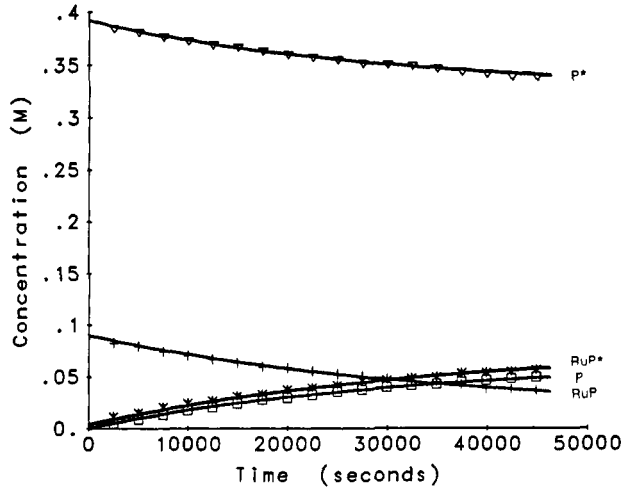

Figure 2. Fit of concentration (M) vs time (seconds) data for phosphine exchange in $Cp^*(PMe_3)_2RuCH_2C_6H_5$ at 100 °C. Data for [Ru–$P(CH_3)_3$], [Ru–$P(CD_3)_3$], [$P(CH_3)_3$](soln) and [$P(CD_3)_3$](soln) shown. Note at long reactions times [Ru–$P(CD_3)_3$] > [$P(CH_3)_3$](soln), reflecting the escape of $P(CH_3)_3$ into the gas phase.

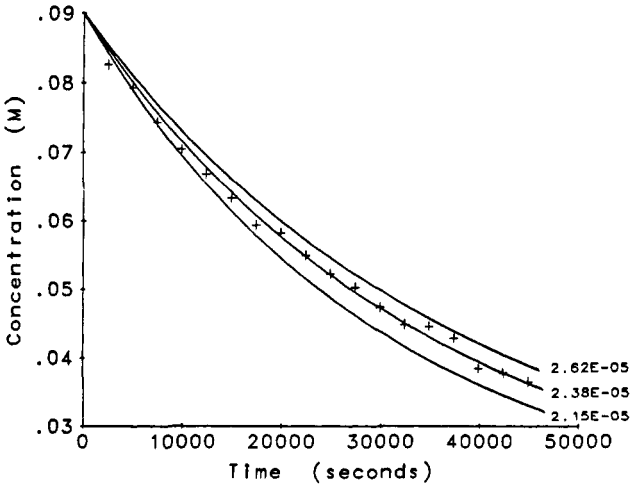

Figure 3. Fit of [Ru–$P(CH_3)_3$] vs time from Figure 2. Solid line reflects best-fit case while other lines reflect the optimized fits when k_1 is fixed at ±10% of the best-fit value and all other rate constants are allowed to reoptimize.

The fit of phosphine exchange data obtained for a representative complex, $Cp^*(PMe_3)_2RuCH_2Ph$, to the kinetic model in eq 4 is shown in Figure 2. Concentrations of all species in this plot were measured directly, or obtained by difference. The intermediate complex [$Cp^*(PMe_3)$-$RuCH_2Ph$] has never been observed in any of our experiments.

By this method, four rate constants were calculated; k_1, k_{-1}, k_2, k_{-2}. As expected, since intermediates are never observed, k_{-1} is not well defined; satisfactory fits to the data are observed as long as $k_{-1} \gg k_1$.[18] However, the fit of the model to the data shown in Figure 2 is very sensitive to the value of k_1. Unsatisfactory fits are obtained when the optimized rate constant k_1 is fixed at ±2% of that optimal value and all other rate constants are reoptimized (Figure 3). This observation suggests the method and data provide values of k_1 which are accurate to better than ±2%.

(15) See Experimental Section of ref 3.
(16) A combination of the standard Nicolet KINET and 1PDNA pulse sequences was used.
(17) GIT was developed as a gear integration package from Havchem by Dr. F. J. Weigert at Du Pont CR&D.
(18) As long as the k_{-1} values were at least 10^6 faster than the dissociation rate the data are adequately explained by the kinetic model. This is reasonable since, while the concentration of the intermediate is never measured, the inability to observe such species indicates they are extremely short lived in the presence of phosphine.

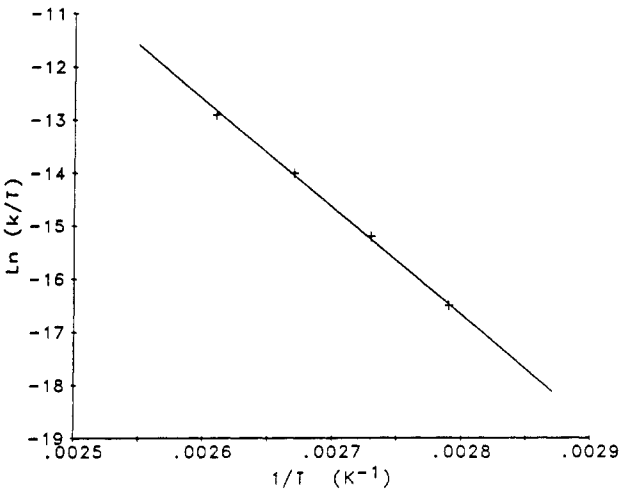

Figure 4. Eyring plot of rate vs temperature data for Cp*-$(PMe_3)_2RuCH_2C_6H_5$.

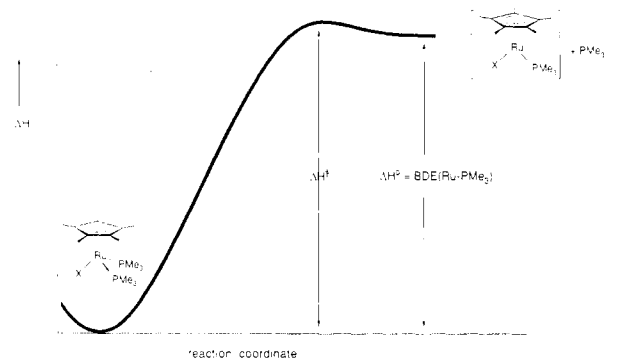

Figure 5. Reaction enthalpy diagram for phosphine dissociation from $Cp^*(PMe_3)_2RuX$. The near-zero activation barrier for the addition of phosphine to $Cp^*(PMe_3)RuX$ suggests the observed activation enthalpy is approximately equivalent to the Ru–P bond dissociation enthalpy.

Treatment of the early part of these data by the method of initial rates gives the same k_1 value to within 10%, as expected when a dissociative mechanism is operating. On the other hand, the method of initial rates gives less exact values of k_1 for the reasons discussed above.

Care must be taken when analyzing data with a modeling program. As is usual for any iterative, multiparameter program, a global minimum must be found. The initial rate guesses must be varied over the widest possible range to show convergence to the same minimum. In addition, in a system of coupled equilibria, such as those in eq 4, care must be taken to avoid program artifacts. The program "GIT" that we have used varies rate constants sequentially, so once the proper ratios of forward and reverse rate constants are found (consistent with K_{eq}), changing the first rate constant will not be productive. GIT will readjust the first rate constant back to the equilibrium value consistent with the second rate constant. However, as can be seen in Figures 2 and 3, with proper care k_1, the rate constant of interest, can be determined quite accurately.

To obtain activation parameters, typically experiments were run over at least a 40 °C range. An Eyring plot of a representative data set is shown in Figure 4.[19] An Arrhenius plot of the data yields the same E_a value as that from the $\Delta H^\ddagger$ value obtained from an Eyring treatment.

(19) As is usual for an Eyring treatment, κ was assumed equal to 1.

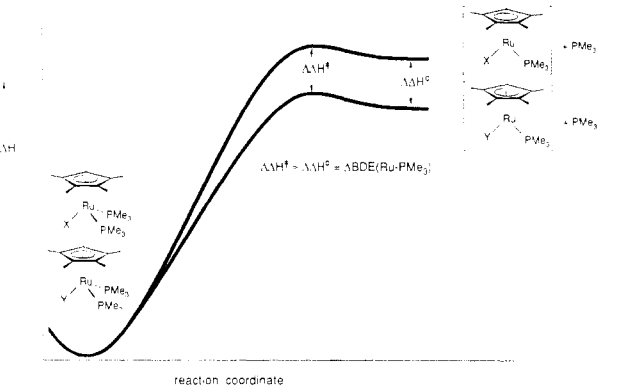

Figure 6. Reaction enthalpy diagram comparing phosphine dissociation from $Cp^*(PMe_3)_2RuX$ to $Cp^*(PMe_3)_2RuY$. As long as the addition of phosphine to unsaturated intermediates has a constant and/or negligible activation barrier, then $\Delta\Delta H^\ddagger \approx \Delta\Delta H°$.

Table I. Activation Parameters for Phosphine Loss from $Cp^*(PMe_3)_2RuX$ Complexes

X	$\Delta H^\ddagger$ (kcal·mol^{-1})[a]	$\Delta S^\ddagger$ (eu)[b]	$\Delta G^\ddagger$ (100 °C) (kcal·mol^{-1})[a,c]
$N(C_6H_5)_2$	23	9	20
NHC_6H_5	28	12	24
OH	29	19	22
SC_6H_5	32	17	26
OC_6H_5	33	26	23
SH	33	21	25
Cl	33	19	26
$CH_2Si(CH_3)_3$	34	22	26
Br	36	29	25
CH_2COCH_3	36	23	27
I	36	23	27
C_6H_5	37	18	30
$CH_2C_6H_5$	38	27	28
CH_3	40	22	32
$C{\equiv}CC_6H_5$	42	22	34
H	>47	(12)	>42[d]

[a] $\Delta H^\ddagger$ and $\Delta G^\ddagger$ values accurate to ±0.5 kcal·mol^{-1}. [b] $\Delta S^\ddagger$ values accurate to ±7 eu. [c] $\Delta G^\ddagger$ values calculated from $\Delta H^\ddagger$ and $\Delta S^\ddagger$ values for T = 100 °C. [d] No exchange of $Cp^*(PMe_3)_2RuH$ with $P(CD_3)_3$ was noted after a week at 187 °C in tetralin-d_{12} indicating, conservatively, that the rate of phosphine dissociation is $<10^{-7}$ s^{-1} (and $\Delta G^\ddagger > 42$ kcal·mol^{-1}) under these conditions. Assuming a conservative $\Delta S^\ddagger$ value of 12 (other $Cp^*(PMe_3)_2RuR$ complexes show $\Delta S^\ddagger = 22 \pm 3$ eu) indicates the $\Delta H^\ddagger$ for dissociation from $Cp^*(PMe_3)_2RuH$ is >47 kcal·mol^{-1}.

Table I lists the activation parameters obtained for all the $Cp^*(PMe_3)_2RuX$ complexes examined. The $\Delta G^\ddagger$ values listed have been extrapolated to a common temperature of 100 °C.[20]

Discussion

Ru–PMe_3 Dative Bond Strengths. We stress that our measurements have not allowed determination of absolute Ru–P BDEs (Figure 5). Nevertheless, if the activation barrier for recombination of free PMe_3 with the 16-electron unsaturated intermediate $[Cp^*(PMe_3)XRu]$ is small and thus essentially constant among this series of complexes, the differences in activation enthalpies ($\Delta\Delta H^\ddagger$) for two complexes should satisfactorily approximate the difference in Ru-PMe_3 bond strengths ($\Delta\Delta H°$) (Figure 6). Support for this premise comes from the large positive free entropies of activation noted for all of these dissociations in-

(20) The Eyring treatment was performed using a program developed locally at Du Pont by R. Farlee and D. C. Roe. The data were fit by using a logarithmic function on the actual data to avoid weighting the data.

Table II. Steric Effects on Activation Barriers for Trimethylphosphine Dissociation from $Cp^*(PMe_3)_2RuX$ Complexes Relative to $Cp^*(PMe_3)_2RuCH_3$

X	$\Delta\Delta H^\ddagger$ (kcal·mol^{-1})	X	$\Delta\Delta H^\ddagger$ (kcal·mol^{-1})
H	>7	$CH_2C_6H_5$	−2
C≡CPh	+2	C_6H_5	−3
CH_3	0	CH_2SiMe_3	−6

dicating the importance of "late" (or product-like) transition states[21] for phosphine loss. This interpretation is also consistent with the observation that $k_{-1}[L] \gg k_1$ for all derivatives.

Steric Effects on Phosphine Dissociation. For ligands, X, which have no significant π interactions with the transition metal, these approximate Ru–P bond strengths can be ordered according to steric bulk, as shown in Table II. Using $cp^*(PMe_3)_2RuCH_3$ as a benchmark for comparison, changing the σ substituent to the small, rodlike phenylacetylide ligand strengthens the Ru–P interactions by about 2 kcal·mol^{-1}. Conversely, when methyl is substituted by a slightly larger ligand, such as benzyl or phenyl, Ru–P bonds weaken by about the same amount. However, when methyl is substituted for a group very much larger (CH_2SiMe_3) or smaller (H), substantial deviations of more than 6 kcal·mol^{-1} in the strengths of Ru–P interactions are indicated.[22]

These observations suggest the functional group additivity approach to organometallic thermochemistry may be quite appropriate when substituents of similar sizes are employed. However, our data indicate that caution must be exercised when thermodynamic investigations involve ligands of dissimilar sizes.[23] This conclusion presupposes that the activation barriers for adding phosphine to $Cp^*(PMe_3)RuCH_3$ and $Cp^*(PMe_3)RuCH_2SiMe_3$ are the same. In fact, the barrier is likely to be larger for adding phosphine to the sterically more congested center (Figure 7) so that the differences in activation barriers for phosphine dissociation represent lower limits for the differences in actual Ru–P bond strengths. Thus our data, as applied to functional group additivity questions, represent a best-case situation. The actual differences in Ru–P bond strengths are likely to be larger than indicated by the data in Table II, and the functional group additivity deviations discussed above may be conservative.

Another way of looking at these data, which involves no assumptions, is that the steric consequences of an ancillary ligand (R) for $Cp^*(PMe_3)_2Ru$-R may have as much as a ±10 kcal·mol^{-1} effect on the activation barrier to phosphine dissociation; i.e., they may exhibit enormously different rates of trimethylphosphine dissociation. In effect, this study quantifies what organometallic chemists have known intuitively for many years: steric changes to a ligated transition-metal complex can dramatically affect the rates of ligand loss.

Electronic Effects on Phosphine Dissociation. The effects of replacing alkyl substituents with ancillary ligands

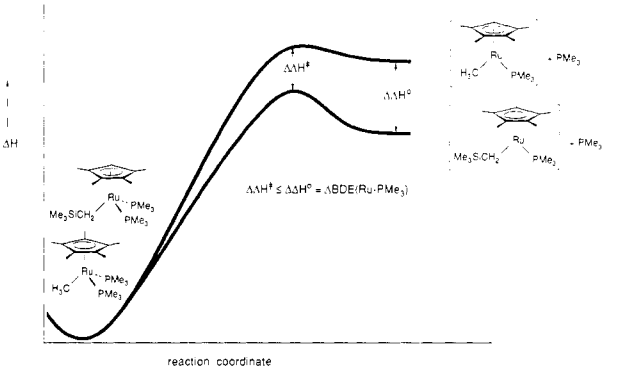

Figure 7. Reaction enthalpy diagram comparing phosphine dissociation from $Cp^*(PMe_3)_2RuCH_3$ to $Cp^*(PMe_3)_2RuCH_2Si(CH_3)_3$. Because the activation barrier for adding phosphine to the sterically more encumbered derivative is higher, $\Delta\Delta H^\ddagger$ is actually less than $\Delta\Delta H$.

Table III. Electronic Effects on Activation Barriers for Trimethylphosphine Dissociation from $Cp^*(PMe_3)_2RuX$ Complexes of Similar Sizes

X	$\Delta H^\ddagger$ (kcal·mol^{-1})	X	$\Delta H^\ddagger$ (kcal·mol^{-1})
CH_3	40	OC_6H_5	33
Cl	33	SC_6H_5	32
SH	33	NHC_6H_5	28
OH	29	I	36
$CH_2C_6H_5$	38	Br	36
CH_2COCH_3	36	Cl	33

X which contain lone electron pairs, yet which are about the same size, are listed in Table III. As can be seen, the relative degree to which π donation from X labilizes a trimethylphosphine ligand of $Cp^*(PMe_3)_2RuX$ roughly parallels the basicity of lone pairs on HX.[24] This π effect can lower $\Delta H^\ddagger$ as much as 10 kcal·mol^{-1} for $Cp^*(PMe_3)_2RuOH$ and $Cp^*(PMe_3)_2RuNHPh$ (vs a comparably sized alkyl). When moving down a triad, as in $Cp^*(PMe_3)_2RuOH$ vs $Cp^*(PMe_3)_2RuSH$ and in the series $Cp^*(PMe_3)_2RuX$ (X = Cl, Br, I), much smaller changes in $\Delta H^\ddagger$ amounting to only 1–2 kcal·mol^{-1} are observed. These relatively small differences may be due to the counterbalancing effects of increased size and reduced π donation of second-row main-group substituents compared to the first-row main-group analogues.[25] The presence of lone electron pairs on the acetone enolate also shows significant ($\Delta\Delta H^\ddagger \approx 3$ kcal·mol^{-1}) reduction in the barrier for PMe_3 loss as compared with a derivative with an alkyl of comparable size.

Although our data do not allow us to attribute the differences in the barriers for phosphine dissociation to differences in the transition state or the ground state (or some of both), it appears more likely that, as shown in Figure 8, the interaction of the lone electron pairs of the σ-bonded lignd X dominates in the transition state. Significant X lone electron pair donation to the highly electron-rich, coordinatively saturated ruthenium center is unlikely. Moreover, we have previously shown from equilibria of the type $Cp^*(PMe_3)_2RuX + HY \rightleftharpoons Cp^*(PMe_3)_2RuY + HX$ that Ru–X bond strengths correlate with H–X bond dissociation energies even when X and/or Y contain electron lone pairs,[3] indicating that no significant

(21) Lowry, T. H.; Richardson, K. S. *Mechanism and Theory in Organic Chemistry*, 2nd ed.; Harper and Row, NY, 1981; 197.

(22) Although there may be differences in ground-state or transition-state hyperconjugative stabilizations due to the different alkyl and hydride ligands, the similarities of Ru–P bond strengths in the ruthenium benzyl, phenyl, methyl, and phenylacetylide complexes suggests any such differences are insignificant compared to the magnitude of changes made by steric differences.

(23) For example, the apparently greater thermodynamic stability of L_nM–H bonds relative to L_nM–CH_3 linkages noted in a number of studies may be due, in large part, to stronger ancillary M–L bonds for hydride complexes relative to those of the methyl analogues. Thus, the higher thermodynamic stabilities for the hydride complexes may not necessarily be due to a particularly strong M–H.

(24) Lias, S. G.; Leibman, J. F.; Levin, R. D. *J. Phys. Chem. Ref. Data* **1984**, *13*, 695.

(25) (a) Buhro, W. E.; Chisholm, M. H.; Folting, K.; Huffman, J. C. *J. Am. Chem. Soc.* **1987**, *109*, 905. (b) McCleverty, J. A. *Chem. Soc. Rev.* **1983**, *12*, 331. (c) Drane, A. S.; McCleverty, J. A. *Polyhedron* **1983**, *2*, 53.

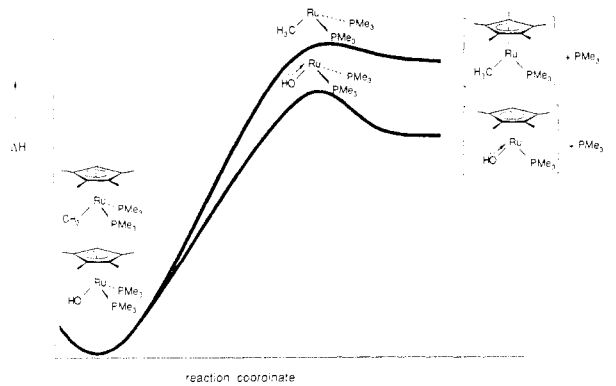

Figure 8. Reaction enthalpy diagram comparing phosphine dissociation from $Cp^*(PMe_3)_2RuCH_3$ to $Cp^*(PMe_3)_2RuOH$ (which shows interaction of a nucleophilic lone electron pair on oxygen with ruthenium as the phosphine dissociates). Since the alkyl derivative has no available nucleophilic lone electron pairs, phosphine dissociation receives no assistance from the neighboring group effects possible in the hydroxide complex.

multiple bonding (arising from X-to-Ru lone-pair donation) between X and Ru occurs for the ground state of these complexes.[26] In fact, the small (ca. 4 kcal·mol^{-1}) span observed in these equilibrium enthalpies may be traced to a combination of factors including: incomplete cancellation of solvation effects, π-back-bonding effects, and changes in σ bonding due to better overlap. Unless significant cancellation of effects is operating, we conclude that the differences in ground-state energies induced by π donation from X must be significantly smaller than this span in equilibrium enthalpy.[3]

While steric interactions have been invoked to explain both metal–alkyl or –hydride BDEs[27] and dative M–L BDEs,[28] ancillary ligand effects of the type presented in this study have apparently not been previously considered. As is evident from the results presented above, the cis ancillary ligand (X) for the pseudooctahedral $Cp^*(PMe_3)_2RuX$ system provides an electronic perturbation on the transition state as large as that induced by steric effects. Such stabilization of the transition state has precedent in organic chemistry. Neighboring groups have been shown to cause large rate increases in the solvolysis of compounds such as alkyl tosylates and halides. The neighboring group displaces the leaving group and stabilizes the resultant carbonium ion, prior to trapping of the intermediate by solvent. Such effects can lead to rate enhancements of 4–10 orders of magnitude.[29]

Neighboring group participation has been invoked previously in the oxidative addition and reductive elimination reactions of square-planar platinum[30] and iridium[31] complexes. Rate enhancements up to ca. 250-fold are observed for complexes containing *o*-methoxyphenyldimethylphosphine and -arsine as compared with the unsubstituted phenyldimethylphosphine and arsine. Interaction of a lone pair on the ligand methoxy group with the transition-metal center in the transition state has been proposed to explain this difference.

The acceleration in the rate of trimethylphosphine dissociation due to lone electron pair donation from the ancillary ligand amounts to roughly six orders of magnitude for $Cp^*(PMe_3)_2RuOH$ as compared to $Cp^*(PMe_3)_2RuCH_3$. The magnitude of this effect is comparable to that found in organic systems. We emphasize again that the magnitude of this electronic effect is comparable to the more commonly invoked steric effects, at least for the $Cp^*(PMe_3)_2RuX$ series.

Conclusions

In summary, activation parameters for PMe_3 dissociation in organoruthenium complexes $Cp^*(PMe_3)_2RuX$ have been determined as the ancillary ligand X is varied, and both steric and electronic effects on the transition for this process have been assessed. A late, product-like transition state is indicated in all cases. With X = hydrocarbyl or hydride, steric bulk appears to determine the relative rate of phosphine loss. When X has lone electron pairs, acceleration of trimethylphosphine dissociation may also occur. This "neighboring group effect" is found to increase rates by ca. 6 orders of magnitude for systems of comparable steric size. Thus, these results provide quantitative evidence for the general perception that both sterics and electronics can play an important role in dative ligand dissociation rates. In addition, the effectiveness of steric congestion in weakening Ru–P bonds suggests great care must be exercised when the functional group additivity assumption is applied to thermochemical investigations in organometallic systems.

Experimental Section

General Considerations. All syntheses and chemical manipulations were carried out in a Vacuum Atmospheres HE-453 drybox equipped with either a nitrogen purge or an oxygen/water scrubbing recirculation "Dri-Train" or by high vacuum and Schlenk techniques.

Benzene-d_6, and toluene-d_8 were purified by vacuum distillation from sodium followed by storage in the drybox over activated (450 °C, 2 h) 4-Å molecular sieves. *O*-Xylene-d_{10}, mesitylene-d_{12}, and tetralin-d_{18} were predried in the drybox over activated molecular sieves but were not distilled from sodium. CD_3I and $^{13}CH_3I$ were used as obtained from Merck. PMe_2Cl was used as obtained from Strem and P(O-*p*-tolyl)$_3$ was used as obtained from Kodak. Dibutyl ether was used as obtained from Aldrich.

NMR spectra were recorded on Nicolet (now GE) NT series spectrometers operating at 300- and 360-mHz proton frequencies, respectively. Variable-temperature measurements were conducted in NMR probes calibrated with a chromel–alumel thermocouple which was, in turn, calibrated at 100 °C and 0 °C with water. Physical measurements were acquired by using Wilmad No. 507-TR screw-capped NMR tubes with Teflon-lined neoprene septa. Tubes were loaded in the drybox by using a Mettler AE160 balance (±0.1 mg) and cold phosphine. Total volume in the tube was calculated from the solution height in these calibrated tubes by using the relationship: volume (μL) = height (mm) × 14.00 + 5.55, which was determined by a least-squares fit of volume vs height data acquired by using Hamilton microliter syringes. T_1s data were acquired with Nicolet (GE) spin-inversion/recovery pulse sequences and data analysis software. A combination of timed kinetic and NOE-suppressed (decoupler on during acquisition, off during recycle) pulse sequences were used to acquire NOE suppressed kinetics information on ligand exchange. A synthetic mixture of $Cp^*(PMe_3)_2RuSH$, $Cp^*(P(CD_3)_3)_2RuSH$, PMe_3, and $P(CD_3)_3$ was used to check the pulse sequence to confirm negligible NOE differences. Spectra were acquired by using 90° pulses with 60-s pulse delays (approximately five T_1s between pulses).

Data were collected by using aromatic deuterated solvents as described above. Benzene-d_6 was used from 20–60 °C while toluene-d_8 was used from 60–90 °C. *O*-Xylene-d_{10} was employed

(26) Except in good π-accepting ligands such as cyanide. In that case evidence for such multiple bonding comes both from infrared data and from a deviation of that bond strength from the H–X/M–X single bond correlation.

(27) Halpern, J. *Inorg. Chim. Acta* **1985**, *100*, 41.

(28) Tolman, C. A. *Chem. Rev.* **1977**, *77*, 313.

(29) Carey, F. A.; Sundberg, R. J. *Advanced Organic Chemistry*; Plenum: New York, 1977; Vol. A, p 229.

(30) Constable, A. G.; Langrick, C. R.; Shabanzadeh, B.; Shaw, B. L. *Inorg. Chim. Acta* **1982**, *65*, L151.

(31) Miller, E. M.; Shaw, B. L. *J. Chem. Soc., Dalton Trans.* **1974**, 480.

from 90 to 120 °C, and mesitylene-d_{12} was the solvent of choice from 120 to 140 °C. Above 140 °C decalin-d_{18} was used. The temperature ranges used to study the individual compounds are listed in Table I.

Concentration vs time data were analyzed by fitting the data to the dissociative kinetic model of this exchange shown in eq 4 using GIT software on a Vax 8650. This software is an iterative program based on the original HAVECHEM[32] programs. Eyring analysis of the kinetics data was done by using ARH2 software[33] on a Vax 8650. This version fits a logarithmic function to the data to avoid artifacts sometimes realized in linear fits of log data. RS/1 software was used to format the data into the expected inputs for these programs.

Synthesis of $^{13}CH_3PMe_3$. This compound was prepared in the drybox. $^{13}CH_3MgI$ was prepared by dissolving Mg into a dibutyl ether solution containing $^{13}CH_3I$. This solution was added to a cold dibutyl ether solution of PMe_2Cl and stirred for 30min as the solution warmed to ambient temperature. The resulting phosphine was distilled twice to remove all traces of butyl ether.

Synthesis of $P(CD_3)_3$. Perdeuteriotrimethylphosphine was prepared by adding a freshly prepared solution of CD_3MgI to tri-*p*-tolyl phosphite in dibutyl ether. The mixture was stirred for an hour at 25 °C, and the resulting phosphine was distilled at atmospheric pressure. The crude phosphine was redistilled to remove all traces of impurities.

Phosphine Exchange Kinetics. In the drybox a screw-capped Wilmad no. 507-Tr 5mm NMR tube was charged with 15–20 mg of $Cp^*(PMe_3)_2RuX$. Benzene-d_6 (approximately 600 μL) was added by pipette, and the tube was capped and reweighed. The entire assembly was cooled in a drybox freezer, along with a 100-μL syringe and $P(CD_3)_3$. After 30 min these items were removed from the freezer. The tube weight was rechecked, then $P(CD_3)_3$ was added, by syringe, and the tube was reweighed. The total solution volume in the tube was determined by height.

The tube was placed in a preequilibrated 40 °C NMR probe and shimmed as thermal equilibrium was attained (approximately 15 min). Spectra were acquired, and the concentrations of species ($Ru-PMe_3$, $Ru-P(CD_3)_3$, PMe_3(soln), and $P(CD_3)_3$(soln) were determined over the same region of each spectrum by an automated series of GR and DR integration routines on the Nicolet spectrometers. The time of each spectrum was similarly recorded along with the data by the internal clock on the spectrometer. This concentration vs time data was simulated with GIT software to obtain the phosphine dissociation rate constant.

Dissociation rates of all th e ruthenium complexes at a variety of temperatures were measured by this same method.

Acknowledgment. We acknowledge the generous financial support of this work by the E. I. du Pont de Nemours and Co., Inc., the Shell Companies Foundation, and the National Science Foundation (Grant No. CHE-8600875). We wish to thank Dr. Don Tilley for carrying out some preliminary measurements of the rates of substitution for some of these compounds. We thank Drs. D. C. Roe and Peter Desrosiers for valuable discussions and assistance in obtaining accurate NMR data and gratefully acknowledge the technical assistance of Joseph H. McCartney and Joseph P. Foster, Jr.

Registry No. $^{13}CH_3PMe_2$, 117309-26-9; $P(CD_3)_3$, 22529-57-3; $^{13}CH_3I$, 4227-95-6; PMe_2Cl, 811-62-1; CD_3MgI, 41251-37-0; $Cp^*(PMe_3)_2Ru(N(C_6H_5)_2)$, 106734-56-9; $Cp^*(PMe_3)_2Ru(NHC_6H_5)$, 106734-55-8; $Cp^*(PMe_3)_2Ru(OH)$, 106734-52-5; $Cp^*(PMe_3)_2Ru(SC_6H_5)$, 117340-64-4; $Cp^*(PMe_3)_2Ru(OC_6H_5)$, 107441-18-9; $Cp^*(PMe_3)_2Ru(SH)$, 106734-57-0; $Cp^*(PMe_3)_2RuCl$, 87640-47-9; $Cp^*(PMe_3)_2Ru(CH_2Si(CH_3)_3)$, 87640-52-6; $Cp^*(PMe_3)_2RuBr$, 87640-48-0; $Cp^*(PMe_3)_2Ru(CH_2COCH_3)$, 106734-54-7; $Cp^*(PMe_3)_2RuI$, 93036-05-6; $Cp^*(PMe_3)_2Ru(C_6H_5)$, 107441-17-8; $Cp^*(PMe_3)_2Ru(CH_2C_6H_5)$, 117340-65-5; $Cp^*(PMe_3)_2Ru(CH_3)$, 87640-49-1; $Cp^*(PMe_3)_2Ru(C{\equiv}CC_6H_5)$, 106734-53-6; $Cp^*(PMe_3)_2RuH$, 87640-53-7; tri-*p*-tolyl phosphite, 620-42-8.

(32) Stabler, R. N.; Chesnick, J. *Int. J. Chem. Kinet.* **1978**, *10*, 461.
(33) Developed at DuPont by R. Farlee and D. C. Roe.

Multinuclear Magnetic Resonance Studies on Substituted Rhodium Carbonyl Clusters

Claudio Allevi, Silvia Bordoni, Charles P. Clavering, Brian T. Heaton,* Jonathan A. Iggo,* and Claudio Seregni

Department of Inorganic, Physical and Industrial Chemistry, University of Liverpool, P.O. Box 147, Liverpool L69 3BX, England

Luigi Garlaschelli

Istituto di Chimica Generale ed Inorganica, Università di Milano, Via G. Venezian 21, 20133 Milano, Italy

Received April 21, 1988

Multinuclear NMR data (^{13}C, ^{31}P, ^{103}Rh, $^{13}C\{^{103}Rh\}$, $^{13}C\{^{31}P\}$, and $^{31}P\{^{103}Rh\}$) for $[Rh_6(CO)_{12}\{P(OPh)_3\}_4]$, $[Rh_6(CO)_{10}(dppm)_3]$, and $(NBu_4)[Rh_6(CO)_{15}X]$ (X = I, CN, or SCN) are presented. The use of $^{13}C\{^{103}Rh\}$ double resonance has allowed the ^{13}CO NMR spectra of $[Rh_6(CO)_{15}I]^-$ and $[Rh_6(CO)_{12}\{P(OPh)_3\}_4]$ to be reassigned. The structures of the clusters in solution have been unambiguously determined. In all cases, the solid-state structure (as determined by X-ray crystallography) is maintained in solution. No evidence for CO exchange on the NMR time scale was found for any of the clusters studied at temperatures below 25 °C. ^{103}Rh NMR data for $[Rh_6(CO)_{15}X]^-$ (X = I, CN, SCN) are compared with those for $[Rh_6(CO)_{16}]$ and $[Rh_6(CO)_{15}H]^-$. Data for the phosphine-substituted derivatives of $[Rh_6(CO)_{16}]$ are compared with those for the ligand-substituted $[Rh_4(CO)_{12}]$ derivatives.

We have previously described the application of $^{13}C\{^{103}Rh\}$ NMR spectroscopy to the determination of the solution structures of $[Rh_4(CO)_{12-x}\{P(OPh)_3\}_x]$ (x = 1–4)[1] and of $[Rh_6(CO)_{15}H]^-$.[2] We now report multinuclear NMR, including $^{13}C\{^{103}Rh\}$ and $^{31}P\{^{103}Rh\}$, studies of Rh_6 clusters $[Rh_6(CO)_{15}X]^-$ (X = I, CN, SCN), $[Rh_6(CO)_{10}(dppm)_3]$, and $[Rh_6(CO)_{12}\{P(OPh)_3\}_4]$. These studies have allowed assignment of the ^{13}C, ^{31}P, and ^{103}Rh NMR spectra

(1) Heaton, B. T.; Strona, L.; Pergola, R. D.; Garlaschelli, L.; Sartorelli, U.; Sadler, I. H. *J. Chem. Soc., Dalton Trans.* **1983**, 173–175.
(2) Heaton, B. T.; Strona, L.; Martinengo, S.; Strumolo, D.; Goodfellow, R. J.; Sadler, I. H. *J. Chem. Soc., Dalton Trans.* **1982**, 1499–1502.

0276-7333/89/2308-0385$01.50/0